

## Nonadiabatic Effects in Resonant Inelastic X-Ray Scattering

F. Hennies,<sup>1,\*</sup> S. Polyutov,<sup>2</sup> I. Minkov,<sup>2</sup> A. Pietzsch,<sup>1</sup> M. Nagasono,<sup>1,3</sup> F. Gel'mukhanov,<sup>2,†</sup> L. Triguero,<sup>4</sup>  
M.-N. Piancastelli,<sup>5</sup> W. Wurth,<sup>1</sup> H. Ågren,<sup>2</sup> and A. Föhlisch<sup>1,\*</sup>

<sup>1</sup>*Institut für Experimentalphysik, Universität Hamburg, Luruper Chaussee 149, D-22761 Hamburg, Germany*

<sup>2</sup>*Theoretical Chemistry, Royal Institute of Technology, AlbaNova University Center, S-106 91 Stockholm, Sweden*

<sup>3</sup>*Department of Materials Science and Engineering, Kyoto University, Sakyo-ku, 606-8501 Kyoto, Japan*

<sup>4</sup>*KTH Syd, Royal Institute of Technology, Campus Haninge, S-136 40 Haninge, Sweden*

<sup>5</sup>*Department of Physics, Uppsala University, Box 530, S-751 21 Uppsala, Sweden*

(Received 11 July 2005; published 10 October 2005)

We have studied the spectral features of resonant inelastic x-ray scattering of condensed ethylene with vibrational selectivity both experimentally and theoretically. Purely vibrational spectral loss features and coupled electronic and vibrational losses are observed. The one-step theory for resonant soft x-ray scattering is applied, taking multiple vibrational modes and vibronic coupling into account. Our investigation of ethylene underlines that the assignment of spectral features observed in resonant inelastic x-ray scattering of polyatomic systems requires an explicit description of the coupled electronic and vibrational loss features.

DOI: [10.1103/PhysRevLett.95.163002](https://doi.org/10.1103/PhysRevLett.95.163002)

PACS numbers: 33.20.Rm, 33.20.Fb, 33.20.Tp, 33.50.Dq

Resonant inelastic x-ray scattering (RIXS), also known as x-ray Raman scattering (RXS), has evolved into a widely used spectroscopic tool to study the electronic structure of matter [1–3]. This development has been promoted by the rapid evolution of high brilliance soft x-ray sources. The Raman selection rule in this photon-in/photon-out spectroscopy gives a high degree of polarization anisotropy and reveals symmetry-information of the systems under investigation. This is also true for the optical dipole transitions underlying the separate x-ray absorption and emission steps. Soft x-ray spectroscopies are element and chemical state selective. In the case of RIXS, these features are strongly enhanced due to the selective excitation of a particular intermediate core-excited state of defined symmetry.

In general, RIXS probes electronic and nuclear (vibrational) inelastic loss processes. In particular, the scattering process is governed by the total symmetry of the coupled nuclear and electronic wave functions. Therefore, strong deviations from a case assuming purely electronic symmetry selection rules have been observed [4,5]. Some studies have addressed the vibrational contributions to the spectral profile, e.g., vibrational broadening [6,7] and lifetime vibrational interference effects [8].

The investigation of condensates and liquids has recently drawn great attention, most prominently the detailed picture of hydrogen bonding in aqueous systems [9,10]. The depth information necessary for such studies makes RIXS ideally suited. In these systems both the geometric configuration and the electronic structure are under debate. The interpretation of the RIXS presented there bases upon the calculation of the electronic spectral states in the adiabatic limit for different molecular configurations which result from molecular dynamics simulations. RIXS spectra, however, contain coupled electronic and vibrational loss features. In this work, we aim

to disentangle the electronic and vibrational contributions to RIXS spectra and investigate the interplay of electronic structure and nuclear dynamics. We have studied RIXS spectral features of condensed ethylene, with vibrational selectivity, in an exemplary way both experimentally and theoretically. We have chosen ethylene as a test system due to its unambiguously characterized electronic and geometric structure [11]. We find in our joint experimental and theoretical investigation that explicit consideration of both the electronic and vibrational loss features is needed to assign spectral states. This is of general relevance for the interpretation of RIXS of any polyatomic system.

The experiments were carried out at MAX-lab, Sweden, on beam line I511-1. Bulk layers of condensed ethylene have been prepared by dosing 100 L onto a *p*-doped silicon substrate cooled to  $\leq 25$  K. The grazing incidence x-ray spectrometer [3] was operated with 0.4 eV bandwidth (full-width-half-maximum FWHM, as all comparable values in this work) in the direction perpendicular to the incident beam axis in magic angle geometry to the electric field vector of the incident radiation. The x-ray absorption spectra (XAS) have been measured with a Scienta SES-200 analyzer in constant final state mode. The excitation bandwidth was set to 35 meV for the x-ray absorption measurement and to 100 meV for RIXS.

The ethylene ( $C_2H_4$ ) molecule has  $D_{2h}$  symmetry and the electronic ground state  $|0\rangle$  configuration is  $(1a_g)^2(1b_{3u})^2(2a_g)^2(2b_{3u})^2(1b_{2u})^2(3a_g)^2(1b_{1g})^2(1b_{1u})^2$ . Ethylene has two symmetry adapted, near-degenerate core orbitals ( $\psi_{\text{core}}:1a_g, 1b_{3u}$ ), which result from the linear combination of the atomically localized C  $1s$  orbitals.  $1b_{1u}$  is the highest occupied molecular orbital (HOMO) and the  $1b_{2g}$  is the lowest unoccupied molecular orbital (LUMO), also called the  $\pi^*$ . The HOMO-LUMO separation is  $\approx 7$  eV.

In our simulations of the resonant x-ray scattering amplitude  $F_{\nu_f}$ , we have included the treatment of multiple vibrational modes and vibronic coupling based on the methods described in Refs. [2,12]. The scattering amplitude  $F_{\nu_f}$  for ethylene is described by the equation (in a.u.):

$$F_{\nu_f} = \frac{1}{2} \sum_{\nu_i} \frac{\Lambda^{(N-N_A)}(\nu_f, \nu_i) [\Lambda_2^{(N_A)}(\nu_f, \nu_i) + \mathcal{P}_f \Lambda_1^{(N_A)}(\nu_f, \nu_i)]}{\omega - \omega_{i\nu_i,00} + i\Gamma/2}. \quad (1)$$

$\hbar\Gamma = 0.1$  eV is the lifetime broadening of the core-excited state,  $\mathcal{P}_f = \pm 1$  the parity of the final electronic state (+ gerade; - ungerade),  $\nu_i = (\nu_{i,1}, \nu_{i,2}, \dots)$  is the vector of the vibrational quantum numbers of all modes of the  $i$ th electronic state, and  $\omega_{i\nu_i, j\nu_j}$  is the electron-vibrational transition energy. We have separated the product of the Franck-Condon (FC) amplitudes  $\Lambda_n^{(N_A)}(\nu_f, \nu_i) = \prod_{q \in A} \langle \nu_{f,q} | \nu_{i,q}; n \rangle \langle \nu_{i,q}; n | 0_{0,q} \rangle$  of  $N_A$  asymmetric vibrational modes, that lead to the localization of the core hole in the  $n$ th carbon atom from the product of the FC amplitudes for the corresponding symmetric vibrational modes  $\Lambda^{(N-N_A)}(\nu_f, \nu_i) = \prod_{q \notin A} \langle \nu_{f,q} | \nu_{i,q} \rangle \langle \nu_{i,q} | 0_{0,q} \rangle$ . The scattering cross section for monochromatic excitation is then given by the equation:

$$\sigma_0(\omega, \omega_1) = \sum_{f, \nu_f} \zeta_{f0} |F_{\nu_f}|^2 \delta(\omega_1 - \omega + \omega_{f\nu_f,00}). \quad (2)$$

$\omega$  and  $\omega_1$  are the frequencies of the incident and scattered photons. The anisotropy factor  $\zeta_{f0} = (d_{fi}^2 d_{i0}^2 / 9) [1 + \frac{1}{10} \times (3\cos^2 \varphi_{f0} - 1)(1 - 3\cos^2 \chi)]$  depends on the angle  $\chi = 35.3^\circ$  between the polarization vector of incident photon and the momentum of the scattered photon (set to the experimental value). The anisotropy factor also depends on the angle  $\varphi_{f0}$  between the transition dipole moments of core excitation  $\mathbf{d}_{i0}$  and emission  $\mathbf{d}_{fi}$ .

Computations of the valence and virtual transition moments were performed in the dipole approximation and have been done within the framework of the density functional theory (DFT) using the STOBE code [13]. The transition energies were taken directly from the Kohn-Sham orbital energies. Numerical analysis of the FC amplitudes reveals that only four in-plane vibrational modes, three  $a_g$  (C-C stretch, H-C-H scissor, and C-H stretch), and one  $b_{3u}$  (C-H asym. stretch), give major contributions to the x-ray absorption and RIXS spectra; therefore, only these four modes were taken into account in the simulations. The FC amplitudes have been computed in the harmonic approximation without consideration of changes in the vibrational frequencies due to the electronic excitations.

In Fig. 1, panel 1 we show the vibrationally resolved x-ray absorption spectrum of ethylene at the  $\pi^*$  resonance, corresponding to the excitation of a  $|\psi_{\text{core}}^{-1} 1b_{2g}\rangle$  electronic state. We can directly assign this vibrational fine structure in agreement with literature [14,15] to the  $a_g$  C-C stretch

vibration and to the  $b_{3u}$  C-H asymmetric stretch vibrational mode. We measured RIXS spectra with the excitation energy tuned onto the vibrational modes of the first core-excited electronic state  $|\psi_{\text{core}}^{-1} 1b_{2g}\rangle$ .

The RIXS spectrum consists of two qualitatively different contributions, namely, the participator or ‘‘elastic’’ band ( $|0\rangle \rightarrow |\psi_{\text{core}}^{-1} 1b_{2g}\rangle \rightarrow |0\rangle$ ) and the spectator or ‘‘inelastic’’ band ( $|0\rangle \rightarrow |\psi_{\text{core}}^{-1} 1b_{2g}\rangle \rightarrow |\psi_f^{-1} 1b_{2g}\rangle$ ) with  $\psi_f = 1b_{1u}, 1b_{1g}, 3a_g, 1b_{2u}$ , denoting valence electronic states. The participator scattering channel leads to the electronic ground state with energy loss features due to vibrational excitations (purely vibrational Raman), while the spectator channel is the scattering to electronically excited final states which is accompanied also by vibrational excitations (vibronic Raman). For clarity of presentation we show the participator RIXS in Fig. 1 and the spectator RIXS in Fig. 2 separately.

Both experiment and theory display a strong dependence of the participator band [Fig. 1, panels (2) and (3)] on excitation energies. For scattering with an incident energy below the resonance energy [Fig. 1(a)], we see mainly a single resonance centered at 0 eV energy loss. This is what is usually referred to as the elastic peak which is the only feature in this channel in the case of single atoms. When exciting on top of the resonance and into higher levels of the vibrational progression [Fig. 1(b)–(f)], the participator profile becomes increasingly asymmetric toward lower energies and a band of inelastic loss features becomes observable. This band moves its center of gravity to lower energies with increasing excitation energy. For the limit of high positive detuning from the electronic resonance we observe decreasing intensity of the vibrational loss features. The cross section for scattering into vibrational excited final states is thus significantly enhanced upon resonant excitation.

The simulations of the participator band are depicted in panel (3) of Fig. 1. We obtain good agreement with the experiment when the simulated spectra are convoluted with a Gaussian of  $\gamma = 0.4$  eV which mimics the total instrumental broadening and excitation bandwidth. Within this envelope we also show the vibrational progression with only  $\gamma = 100$  meV broadening. The spacing of the vibrational states corresponds to the electronic ground state vibrational modes. The intensities of the vibrational loss features are governed by the Kramers-Heisenberg scattering amplitude [Eq. (1)]. The lifetime vibrational interference influences strongly the spectral profile [16]. In particular, we find both in experiment and theory that the detuning  $\Omega = \omega - \omega_{i0,00}$  of the incident photon energy from the electronic  $\pi^*$  resonance leads to only a single spectral line. The origin of this collapse of the vibrational structure is the shortening of the scattering duration [17]  $\tau_{\text{eff}} = 1/\sqrt{\Gamma^2 + \Omega^2}$  with increase of  $|\Omega|$ . A short scattering duration will not allow the nuclear wave packet to dynamically evolve [2,18], thus effectively suppressing

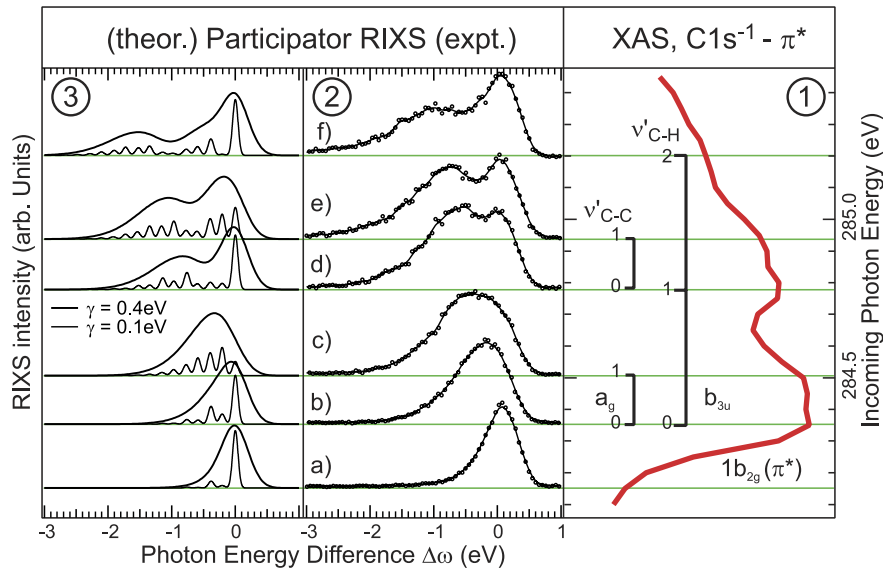


FIG. 1 (color online). Participator RIXS of ethylene at the C K edge (final state is electronic ground state). Panel (1): C  $1s \rightarrow \pi^*$  absorption spectrum; (2) RIXS spectra (expt.) with excitation at the energies indicated; (3) simulated RIXS at the according energies. RIXS spectra are plotted vs the energy difference of outgoing and incoming photon  $\Delta\omega = \omega_1 - \omega$ .

vibrational motion during the scattering and letting vibrational contributions to the spectral profile vanish.

The physics of the formation of the spectator scattering channel is rather different from the participator scattering channel. The spectator channel corresponds to scattering into four different electronic final states:  $|1b_{1u}^{-1}1b_{2g}\rangle$ ,  $|1b_{1g}^{-1}1b_{2g}\rangle$ ,  $|3a_g^{-1}1b_{2g}\rangle$ , and  $|1b_{2u}^{-1}1b_{2g}\rangle$ . The scattering to the ungerade final states ( $|1b_{1u}^{-1}1b_{2g}\rangle$ ,  $|1b_{2u}^{-1}1b_{2g}\rangle$ ) is forbidden according to the parity selection rules. However, the experiment as well as the theory (Fig. 2) show the breakdown [19] of these selection rules when exciting resonantly into the  $\pi^*$  and its vibrational progression [Fig. 2(b)–2(f)]. The origin of this effect is the mixing of near-degenerate gerade and ungerade core-excited states ( $|1b_{3u}^{-1}1b_{2g}\rangle$ ,  $|1a_g^{-1}1b_{2g}\rangle$ ) by the activation of the ungerade  $b_{3u}$  vibration, effectively localizing the core-excited state. We clearly can see the restoration of the selection rules for large detuning [Fig. 2(a)], i.e., the quenching of the symmetry forbidden transitions. This “purification” of the spectator spectrum happens due to the shortening of the scattering duration, leaving no time for the  $b_{3u}$  vibration to mix the core-excited states with different parities [5]. If the detuning is sufficiently large, the spectator RIXS [Fig. 2(a)] is restricted to the electronic final states  $|3a_g^{-1}1b_{2g}\rangle$  and  $|1b_{1g}^{-1}1b_{2g}\rangle$ .

Taking vibronic coupling into consideration, our theoretical approach can fully describe all spectral features in the RIXS spectra (Fig. 2). In particular, the nominal adiabatic transition, defined by the purely electronic transitions, can become very small in comparison to the vibrationally excited final states. Taking spectra in Fig. 2(d)–

2(f) as an example, we can illustrate how crucial it is to take the full vibronic spectral profile into consideration in the interpretation of experimental RIXS. For the electronically excited final states, we observe vibrational progressions extending over 2 eV  $\sim$  4 eV, with a bimodal vibrational envelope. Moreover, the spectral shape of each excited final state changes with photon energy [Fig. 2(d)–2(f)] significantly and differently for each of them.

In summary, we have studied RIXS spectral features of condensed ethylene with vibrational selectivity, both experimentally and theoretically. The theoretical model of the inelastic scattering process takes multiple vibrational modes and vibronic coupling into account. We have obtained excellent agreement between experiment and simulations for the purely vibrational spectral loss features in the RIXS participator channel, reaching the electronic ground state as a final state. We have also observed the coupled electronic and vibrational loss features of the spectator RIXS channel, reaching electron-hole final states combined with vibrational excitation. We have disentangled these contributions and investigated the interplay of electronic structure and nuclear dynamics in an exemplary way. We find the excited electronic final states to split significantly into broad vibrational bands with a complicated, partly bimodal, envelope structure. This goes beyond the spectral distribution expected from an adiabatic model, where vibronic effects are only implicitly treated in a broadening of states. In conclusion, we find that the explicit consideration of coupled electronic and vibrational states in the one-step theory of resonant inelastic x-ray scattering is required to fully assign RIXS spectral states of ethylene.

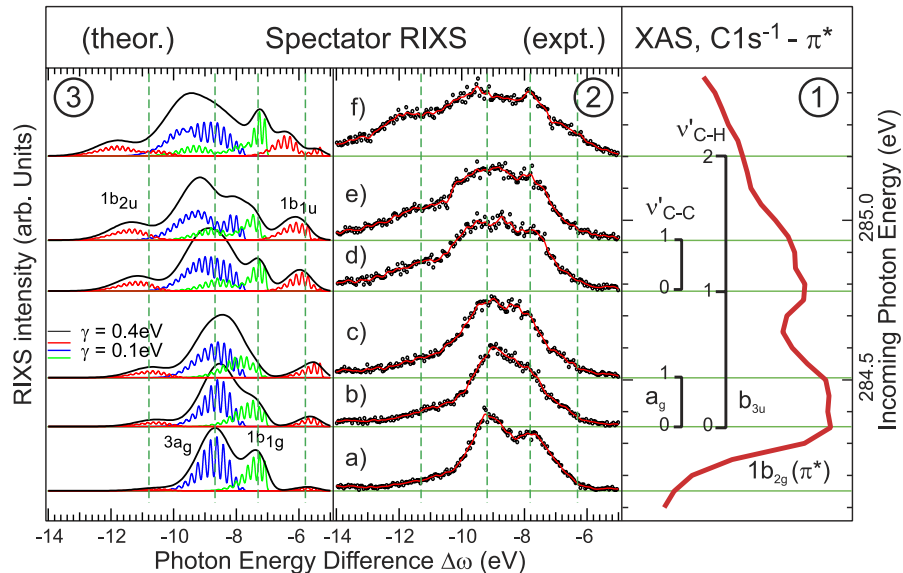


FIG. 2 (color online). Spectator RIXS of ethylene at the C  $K$  edge (final state is valence electronic excited). Panel (1): C  $1s \rightarrow \pi^*$  absorption spectrum; (2) RIXS spectra (expt.) with excitation at the energies indicated; (3) simulated RIXS spectra at the according energies. RIXS spectra are plotted vs the energy difference of outgoing and incoming photon  $\Delta\omega = \omega_1 - \omega$ .

This work was supported by the Access to Research Infrastructure (ARI) Program of the EU, the Swedish National Research council (VR) and the Deutsche Forschungsgemeinschaft (Grant No. DFG Fo343/1-1). M.N. acknowledges support from MEXT Japan, Grant in Aid for Young Scientists (B) 2003. Valuable support from Lisbeth Kjeldgaard and MAX-lab staff is gratefully acknowledged.

\*Electronic address: alexander.foehlich@desy.de; franz@hennies.org

†Permanent address: Institute of Automation and Electrometry, 630090 Novosibirsk, Russia.

- [1] A. Föhlisch, M. Nyberg, J. Hasselström, O. Karis, L. G. M. Pettersson, and A. Nilsson, *Phys. Rev. Lett.* **85**, 3309 (2000).
- [2] F. Gel'mukhanov and H. Ågren, *Phys. Rep.* **312**, 87 (1999).
- [3] J. Nordgren and J. Guo, *J. Electron Spectrosc. Relat. Phenom.* **110-111**, 1 (2000).
- [4] K. Gunnelin, P. Glans, J.-E. Rubensson, C. Sâthe, J. Nordgren, Y. Li, F. Gel'mukhanov, and H. Ågren, *Phys. Rev. Lett.* **83**, 1315 (1999).
- [5] P. Skytt, P. Glans, J.-H. Guo, K. Gunnelin, C. Sâthe, J. Nordgren, F.K. Gel'mukhanov, A. Cesar, and H. Ågren, *Phys. Rev. Lett.* **77**, 5035 (1996).
- [6] Y. Harada, T. Tokushima, Y. Takata, T. Takeuchi, Y. Kitajima, S. Tanaka, Y. Kayanuma, and S. Shin, *Phys. Rev. Lett.* **93**, 017401 (2004).
- [7] Y. Ma, P. Skytt, N. Wassdahl, P. Glans, D.C. Mancini, J. Guo, and J. Nordgren, *Phys. Rev. Lett.* **71**, 3725 (1993).
- [8] P. Skytt, P. Glans, K. Gunnelin, J. Guo, and J. Nordgren, *Phys. Rev. A* **55**, 146 (1997).
- [9] J.-H. Guo, Y. Luo, A. Augustsson, S. Kashtanov, J.-E. Rubensson, D. Shuh, H. Ågren, and J. Nordgren, *Phys. Rev. Lett.* **91**, 157401 (2003).
- [10] M. Odelius *et al.*, *Phys. Rev. Lett.* **94**, 227401 (2005).
- [11] A. J. Merer and R. S. Mulliken, *Chem. Rev.* **69**, 639 (1969).
- [12] F. Gel'mukhanov, T. Privalov, and H. Ågren, *Zh. Eksp. Teor. Fiz.* **112**, 37 (1997) [*JETP* **85**, 20 (1997)].
- [13] STOBE-DEMON Version 1.0, K. Hermann and L. G. M. Pettersson, M. E. Casida, C. Daul, A. Goursot, A. Koester, E. Proynov, A. St-Amant, and D. R. Salahub. Contributing authors: V. Carravetta, H. Duarte, N. Godbout, J. Guan, C. Jamorski, M. Leboeuf, V. Malkin, O. Malkina, M. Nyberg, L. Pedocchi, F. Sim, L. Triguero, and A. Vela, STOBE Software, 2002, <http://w3.rz-berlin.mpg.de/~hermann/StoBe/index.html>
- [14] F. X. Gadea, H. Köppel, J. Schirmer, L. S. Cederbaum, K. J. Randall, A. M. Bradshaw, Y. Ma, F. Sette, and C. T. Chen, *Phys. Rev. Lett.* **66**, 883 (1991).
- [15] Y. Ma, F. Sette, G. Meigs, S. Modesti, and C. T. Chen, *Phys. Rev. Lett.* **63**, 2044 (1989).
- [16] F. K. Gel'mukhanov, L. N. Mazalov, and A. V. Kondratenko, *Chem. Phys. Lett.* **46**, 133 (1977).
- [17] F. Gel'mukhanov, T. Privalov, and H. Ågren, *Phys. Rev. A* **56**, 256 (1997).
- [18] F. Gel'mukhanov, P. Salek, T. Privalov, and H. Ågren, *Phys. Rev. A* **59**, 380 (1999).
- [19] W. Domcke and L. S. Cederbaum, *Chem. Phys.* **25**, 189 (1977).